Available online at www.sciencedirect.com
ScienceDirect
Biomaterials 29 (2008) 709–723
Biomaterials
www.elsevier.com/locate/biomaterials

Development of lipid particles targeted via sugar–lipid conjugates as novel nuclear gene delivery system

Tomoya Masuda[a,c], Hidetaka Akita[a,c,*], Takashi Nishio[b], Kenichi Niikura[b], Kentaro Kogure[a,c], Kuniharu Ijiro[b], Hideyoshi Harashima[a,c]

[a]*Faculty of Pharmaceutical Sciences, Hokkaido University, Kita 12 Nishi 6, Kita-Ku, Sapporo, Hokkaido 060-0812, Japan*
[b]*Research Institute for Electronic Science, Hokkaido University, Kita 21 Nishi 10, Kita-Ku, Sapporo, Hokkaido 001-0021, Japan*
[c]*CREST, Japan Science and Technology Agency, Japan*

Received 16 May 2007; accepted 28 September 2007
Available online 14 November 2007

Abstract

Efficient nuclear gene delivery is essential for successful gene therapy. This study developed a novel system that mimics the mechanism of nuclear entry of adenovirus (Ad) by means of a Multifunctional Envelope-type Nano Device (MEND). In this system, plasmid DNA (pDNA) was condensed with polycation, followed by encapsulation in a lipid membrane. To target MEND to the nuclear pore complex (NPC), sugar served as a NPC-mediated nuclear targeting device was modified on the surface of the lipid envelope. This was accomplished via synthesis of a sugar–cholesterol conjugate. After binding of the MEND to the NPC, the pDNA core was transferred into the nucleus in conjunction with a breakdown of the lipid envelope. Sugar-modified MEND showed higher transfection efficiency compared with unmodified MEND, in non-dividing and dividing cells. Confocal microscopy confirmed that nuclear transfer of pDNA was improved by sugar modification of MEND. Furthermore, destabilization of the lipid envelope significantly enhanced transfection activity: therefore, nuclear-delivery efficiency was closely related to lipid envelope stability. Moreover, quantitative evaluation of cellular uptake and nuclear transfer processes by real-time PCR confirmed that the surface sugars affected nuclear transfer, but not cellular uptake. In summary, a novel system for the nuclear delivery of pDNA was successfully developed by using a sugar-modified MEND and by optimizing the lipid envelope stability.

Keywords: Non-viral vector; Gene delivery; Nuclear delivery; Sugar; Envelope-type nano device

1. Introduction

Nuclear transport of therapeutic genes is a primary limiting step in intracellular trafficking of gene vectors. In dividing cells, disappearance of the nuclear membrane during cell division allows plasmid DNA (pDNA) to be transported into the nucleus. However, in non-dividing cells, the nuclear membrane is the ultimate barrier that limits migration of pDNA into the nucleus. Because non-dividing cells compose a large part of living organisms, development of an efficient nuclear gene delivery system is an important breakthrough towards realizing successful gene therapy [1–6].

Many attempts have been made to overcome the nuclear membrane barrier using functional devices, commencing with the nuclear localization signal (NLS) derived from SV40 Large T antigen. Strategies used in these attempts are classified roughly into two types: (i) direct conjugation of NLS to DNA [7–11], and (ii) electrostatic interaction between DNA and cationic amino acids in NLS [12–16]. Although enhancement of transgene expression was observed in the latter case, these strategies may not be ideal due to difficulties controlling the topology and density of NLS. Therefore, for efficient nuclear gene delivery, more sophisticated strategies are desired.

Some viruses, such as adenovirus (Ad), influenza virus, herpes virus, SV40, and HIV possess sophisticated

*Corresponding author. Faculty of Pharmaceutical Sciences, Hokkaido University, Kita 12 Nishi 6, Kita-Ku, Sapporo, Hokkaido 060-0812, Japan. Tel.: +81 11 706 3735; fax: +81 11 706 4879.
E-mail address: akita@pharm.hokudai.ac.jp (H. Akita).

0142-9612/$ - see front matter © 2007 Elsevier Ltd. All rights reserved.
doi:10.1016/j.biomaterials.2007.09.039

mechanisms for transporting their genome into the nucleus of host cells [17]. It is well known that Ad delivers its genomic DNA to a wide range of cell lines not only in dividing, but also in non-dividing, cells. Therefore, adenoviral vectors are widely used as a tool for gene delivery [18,19]. In addition, the mechanism of Ad nuclear entry has been thoroughly investigated (Fig. 1A). After Ad is incorporated into host cells, it travels through the cytoplasm and binds to the nuclear pore complex (NPC) with the aid of microtubule machinery. The proximity of the Ad capsid to the NPC allows hexon binding to histone H1. The hexon–histone H1 complex then is transported into the nucleus by histone H1 import factors (i.e. importin 7 and importin β). This triggers a nuclear transfer of Ad genomic DNA in conjunction with disruption of the viral capsid [20].

In the present study, a nuclear gene delivery system was developed based on the novel concept of a "degradable lipid envelope on the NPC," which mimics the mechanism of adenoviral nuclear entry, but uses a non-viral gene vector (Fig. 1B). In this study, a Multifunctional Envelope-type Nano Device (MEND), in which pDNA was condensed with polycation, followed by encapsulation with lipid envelope, was used as the vector. MEND is advantageous because they can be modified with functional devices on the surface of the lipid envelope [21–23]. In the present study, MEND modified with octaarginine (R8) (R8-MEND), was prepared from stearylated R8 (STR-R8). R8 induces cellular uptake via macropinocytosis. This pathway is advantageous because it avoids a lysosomal degradation and releases its cargo into the cytoplasm [24,25]. Development of a novel nuclear-delivery system requires the ability to control nuclear targeting and subsequent destabilization of the lipid envelope (Fig. 1B). To target MEND to the NPC, NLS must be displayed on the surface. In this study, sugars were used as the nuclear targeting ligands.

Acquisition of nuclear transfer ability by sugar modification was first reported by Duverger et al. [26]. They reported that sugar-conjugated bovine serum albumin

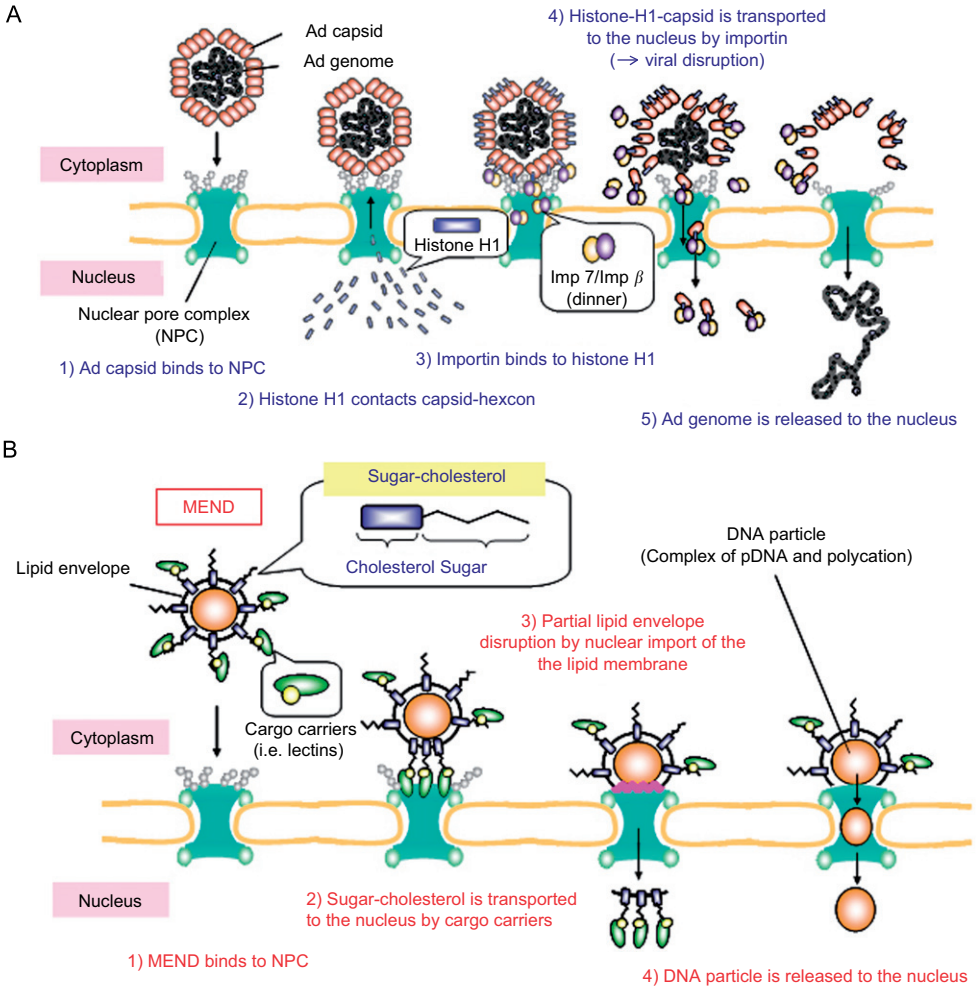

Fig. 1. Schematic diagram illustrating the strategy for nuclear entry of Ad and a novel strategy for the efficient nuclear delivery of plasmid DNA. After binding to NPC by means of NLSs of capsid proteins, Ad releases its genome core into the nucleus in conjunction with disruption of viral structure (A). In the present study, an efficient nuclear gene delivery system, which mimics the nuclear entry of Ad, was developed based on a novel concept of a "degradable lipid envelope on the nuclear pore complex" (B).

(BSA) accumulated in large amounts in the cell nucleus. In resent decades, the function of sugar molecules as a nuclear transport signal has been clarified [27–29]. According to these reports, sugar-dependent nuclear transport was mediated by its receptors (i.e. lectins) and occurred in an energy-dependent manner via NPC. Moreover, since this pathway was not inhibited by an excess of NLS peptides, the sugar-mediated pathway was quite different from the NLS-mediated pathway. These reports also revealed sugar-specificity in nuclear delivery. Nuclear delivery of BSA modified with glucose, mannose, *N*-acetylglucosamine (GlcNAc), and fucose was clearly observed; in contrast, modification with galactose, lactose, and 6-phospomannose did not enhance nuclear delivery. Therefore, sugar molecules may be good candidates for nuclear targeting signals of gene vectors.

To permit sugar-display on the surface of the MEND, the sugars were conjugated to cholesterol, and the sugar–cholesterol conjugates then were anchored to the lipid envelope via the cholesterol moiety. The present study addresses the utility of the novel nuclear-delivery system by measuring transgene expression and nuclear transfer of pDNA in non-dividing (synchronized) cells.

2. Materials and methods

2.1. Materials

pDNA encoding EGFP-luc (6,367) encoding the EGFP-luciferase fusion protein was purchased from Clontech (Palo Alto, CA, USA). The pDNA was purified with a Qiagen Endfree plasmid Mega Kit (Qiagen GmbH, Hilden, Germany). Protamine sulfate salmon mint was purchased from Calbiochem (Darmstadt, Germany). Cholesterol, 1,2-dioleoyl-*sn*-glycero-3-phosphoethanolamine (DOPE), and 1,2-Dioleoyl-*sn*-glycero-3-phosphoethanolamine-*N*-(7-nitro-2-1,3-benzoxadiazole-4-yl) (NBD-DOPE) were purchased from Avanti Polar Lipids, Inc. (Alabaster, AL, USA). Stearylated octaarginine (STR-R8) was synthesized as described previously [30]. Tetramethylrhodamine-labeled dextran (Rho-dex, MW: 70,000) was purchased from Molecular Probes (Eugene, OR, USA). Hydroxyurea, Hoechst 33342, *N*-acetylglucosamine (GlcNAc), mannose, and galactose were purchased from Sigma (St. Louis, MO, USA). Heparin sodium was obtained from Wako (Osaka, Japan).

2.2. Synthesis of sugar–cholesterol conjugates

2.2.1. Cholest-5-en-3β-ol-p-toluenesulfonate (1)

A solution of cholest-5-en-3β-ol (10 g, 25.86 mmol) and *p*-toluenesulfonylchloride (10 g, 52.47 mmol) in dry pyridine (100 ml) was stirred for 16 h at room temperature. After addition of water (25 ml) to the reaction, the mixture was extracted with chloroform (50 ml, three times). The organic phase was dried over anhydrous sodium sulfate and concentrated *in vacuo*. The residue was purified by flash SiO_2 column chromatography with elution of $CHCl_3$/EtOAc (9:1) to give compound **1** as a white powder (78% yield). ^{1}H NMR (400 MHz, $CDCl_3$) δ/ppm: 7.81 (d, 2H, $J = 8.3$ Hz), 7.35 (d, 2H, $J = 8.5$ Hz), 5.33 (d, 1H, $J = 5.3$ Hz), 4.30–4.41 (m, 1H), 1.62 (s, 3H), 0.98 (s, 3H), 0.91 (d, 3H, $J = 7.6$ Hz), 0.89 (d, 6H, $J = 7$ Hz), 0.69 (s, 3H).

2.2.2. 11-(cholest-5-en-3β-yloxy)-3,6,9-trioxaundecan-1-ol (2)

Tetraethyleneglycol (2.00 g, 10.3 mmol) was added to a solution of compound **1** (1.00 g, 18.0 mmol) in 1,4-dioxane (18 ml). The mixture was refluxed for 4 h. The reaction mixture was concentrated *in vacuo*, and the residue was purified by flash SiO_2 column chromatography with elution of $CHCl_3$/EtOAc/MeOH (8:1:1) to give compound **2** as a yellow syrup (80% yield). ^{1}H NMR (400 MHz, $CDCl_3$) δ/ppm: 5.32 (m, 1H), 3.55–3.75 (m, 16H), 3.12–3.23 (m, 1H), 1.75–2.43 (m, 7H), 0.82–1.72 (m, 33H), 0.68 (s, 3H). MALDI-TOF MS: $[M + Na]^+$ 585.17 (obsd), 585.85 (calcd).

2.2.3. 11-(Cholest-5-en-3β-yloxy)-3,6,9-trioxaundecanyl-3,4,5-tri-O-acetyl-2-N-troc-β-D-glucopyranoside (3)

A mixture of 3,4,5-tri-*O*-acetyl-1-thiophenyl-2-*N*-troc-β-D-glucopyranoside (240 mg, 0.640 mmol), compound **2** (120 mg, 0.21 mmol), *N*-iodosuccinimide (140 mg, 0.640 mmol), and molecular sieve 4 Å in dry CH_2Cl_2 (10 ml) was stirred for 10 min at −20 °C, and then trifluoromethane sulfonic acid (10 μl) was added. The mixture was stirred for 0.5 h at −20 °C and reaction temperature gradually was raised to room temperature. After the reaction finished, a drop of triethylamine was added to the mixture. The mixture was diluted with CH_2Cl_2, filtered, and washed with saturated Na_2SO_4 and brine. The solution was concentrated under reduced pressure and purified by silica gel chromatography ($CHCl_3$/EtOAc = 6.5:3.5). Compound **3** was obtained as a white syrup (59% yield). ^{1}H NMR (400 MHz, $CDCl_3$) δ/ppm: 6.53 (d, 1H, $J = 9.1$ Hz), 5.32 (m, 1H), 5.22 (m, 1H), 5.10 (m, 1H), 4.65–4.90 (m, 2H), 4.57 (d, 1H, $J = 11.9$ Hz), 4.13–4.32 (m, 2H), 3.55–3.92 (m, 16H), 3.13–3.18 (m, 1H), 2.73 (d, 3H, $J = 17.9$ Hz), 2.32–2.38 (m, 2H), 2.5–2.23 (m, 2H), 1.94–2.14 (m, 9H), 1.76–1.91 (m, 1H), 0.82–1.72 (m, 33H), 0.66(s, 3H). MALDI-TOF MS: $[M + Na]^+$ 1048.06 (obsd), 1048.51 (calcd).

2.2.4. 11-(Cholest-5-en-3β-yloxy)-3,6,9-trioxaundecanyl-2-N-acetyl-β-D-glucopyranoside (4)

Acetic anhydride (3 ml, 27.20 mmol), acetic acid (3 ml, 47.62 mmol), and activated zinc powder (Zn–Cu, activated by 100 mM $CuSO_4 \cdot 5H_2O$, catalytic amount) were added to a solution of compound **3** (130 mg, 0.120 mmol) in THF (5 ml). The reaction mixture was stirred for 5 h at room temperature. After filtering the zinc powder, the mixture was diluted with CH_2Cl_2, washed with water and concentrated *in vacuo*. The residue was dissolved in methanol (20 ml); sodium methoxide was added (28% solution of methanol, 19 μl, 99 nmol), and the mixture was stirred for 1 h at room temperature. After neutralization with DOWEX (50WX8-200) and filtration, the mixture was concentrated *in vacuo* and purified by silica gel chromatography ($CHCl_3$/EtOAc/MeOH = 7:2:1). Compound **4** was obtained as a white syrup in 19% yield (30 mg, 39.1 μmol). ^{1}H NMR (400 MHz, MeOH-d_4) δ/ppm: 5.35 (d, $J = 1.1$ Hz, 1H), 4.48 (d, $J = 8.5$ Hz, 1H), 3.82–3.98 (m, 2H), 3.56–3.78 (m, 18H), 3.42 (t, $J = 8.3$ Hz, 1H), 3.19 (m, 1H), 2.34 (m, 1H), 1.70–2.25 (m, 8H), 0.28–1.68 (m, 38H). MALDI-TOF MS: $[M + Na]^+$ 787.69 (obsd), 788.53 (calcd).

2.2.5. 11-(Cholest-5-en-3β-yloxy)-3,6,9-trioxaundecanyl-2,3,4,6-tetra-O-acetyl-α-D-mannopyranoside (5)

To a solution of **2** (1.0 g, 1.7 mmol) in dry CH_2Cl_2 (10 ml), 1,2,3,4,6-penta-*O*-acetyl-α-D-mannopyranoside (1.0 g, 2.20 mmol) and boron trifluoride ethyl ether complex (1.2 g, 8.40 mmol) was added and the mixture was stirred for 16 h at room temperature. After dilution with $CHCl_3$, the mixture was washed with a saturated solution of $NaHCO_3$ and water. The organic layer was concentrated *in vacuo* and purified by silica gel chromatography ($CHCl_3$/EtOAc = 6.5:3.5). Compound **5** was obtained as a white syrup in 3% yield (40 mg, 44.8 μmol). ^{1}H NMR (400 MHz, $CDCl_3$) δ/ppm: 5.39 (d, $J = 2.7$ Hz, 1H), 5.34 (m, 1H), 5.22 (dd, $J = 7.9$, 10.4 Hz, 1H), 4.95–5.10(m, 1H), 4.57 (d, $J = 7.9$ Hz, 1H), 4.16 (m, 1H), 3.40–3.98 (m, 1H), 3.65 (m, 16H), 3.12–3.23 (m, 1H), 2.32–2.48 (m, 2H), 1.90–2.20 (m, 15H), 0.56–1.60 (m, 35H), 0.67 (s, 3H). MALDI-TOF MS: $[M + Na]^+$ 914.26 (obsd), 915.54 (calcd).

2.2.6. 11-(Cholest-5-en-3β-yloxy)-3,6,9-trioxaundecanyl-α-D-mannopyranoside (6)

To a solution of **5** (40 mg, 44.8 μmol) in methanol (20 ml), sodium methoxide (28% solution of methanol, 10 μl, 52 nmol) was added, and the mixture was stirred for 1 h at room temperature. After neutralization with DOWEX (50WX8-200) and filtration, the mixture was concentrated

in vacuo and purified by silica gel chromatography ($CHCl_3$/EtOAc/MeOH = 6:3:1). Compound **6** was obtained as a white syrup in 98% yield (32 mg, 44.1 μmol). ^{1}H NMR (400 MHz, MeOH-d_4) δ/ppm: 5.30–5.42 (m, 1H), 5.02–5.09 (m, 1H), 1.79 (m, 1H), 1.73 (m, 1H), 3.52–3.88 (m, 18H), 3.16–3.26 (m, 1H), 2.33–2.52 (m, 1H), 2.11–2.24 (m, 1H), 1.80–2.10 (m, 3H), 0.58–1.55 (m, 33H), 0.64–0.76 (m, 3H). MALDI-TOF MS: $[M+Na]^+$ 746.83 (obsd), 747.50 (calcd).

2.2.7. 11-(Cholest-5-en-3β-yloxy)-3,6,9-trioxaundecanyl-2,3,4,6-tetra-O-acetyl-β-D-galactopyranoside (7)

To a solution of **2** (1.00 g, 1.70 mmol) in dry CH_2Cl_2 (10 ml), 1,2,3,4,6-penta-*O*-acetyl-β-D-galactopyranoside (1.00 g, 2.20 mmol) and boron trifluoride ethyl ether complex (1.20 g, 8.40 mmol) was added. The mixture was stirred for 16 h at room temperature. After dilution with $CHCl_3$, the mixture was extracted with a saturated solution of $NaHCO_3$ (100 ml) and deionized water (100 ml). The organic phases were concentrated *in vacuo* and purified by silica gel chromatography ($CHCl_3$/EtOAc = 6.5:3.5). Compound **7** was obtained as a white syrup in 2% yield (32 mg, 35.8 μmol). ^{1}H NMR (400 MHz, $CDCl_3$) δ/ppm: 5.39 (d, $J = 2.7$ Hz, 1H), 5.34 (m, 1H), 5.22 (dd, $J = 7.9$ Hz, 10.4 Hz, 1H), 4.95–5.10 (m, 1H), 4.57 (d, $J = 7.9$ Hz, 1H), 4.16 (m, 1H), 3.40–3.98 (m, 1H), 3.65 (m, 16H), 3.12–3.23 (m, 1H), 2.32–2.48 (m, 2H), 1.90–2.20 (m, 15H), 0.56–1.60 (m, 35H), 0.67(s, 3H). MALDI-TOF MS: $[M+Na]^+$ 914.39 (obsd), 915.54 (calcd).

2.2.8. 11-(Cholest-5-en-3β-yloxy)-3,6,9-trioxaundecanyl-β-D-galactopyranoside (8)

To a solution of **7** (32 mg, 35.8 μmol) in methanol (20 ml), sodium methoxide (28% solution of methanol, 10 μl, 52 nmol) was added, and the mixture was stirred for 1 h at room temperature. After neutralization with DOWEX (50WX8-200) and filtration, the mixture was concentrated *in vacuo* and purified by silica gel chromatography ($CHCl_3$/EtOAc/MeOH = 7:1:2). Compound **8** was obtained as a syrup in 80% yield (20.8 mg, 28.7 μmol). ^{1}H NMR (400 MHz, $CDCl_3$) δ/ppm: 5.36 (d, $J =$ 5.1 Hz, 1H), 4.25 (d, $J = 7.3$ Hz, 1H), 3.95–4.07 (m, 1H), 3.87 (d, $J =$ 3.2 Hz, 1H), 3.68–3.70 (m, 6H), 3.57–3.68 (m, 14H), 3.40–3.58 (m, 4H), 3.20 (m, 1H), 2.38 (d, $J = 15.2$ Hz 1H), 2.18 (t, $J = 11.3$ Hz, 1H), 1.80–2.08 (m, 3H), 0.80–1.64 (m, 34H), 0.73 (s, 3H). MALDI-TOF MS: $[M+Na]^+$ 746.72 (obsd), 747.50 (calcd).

2.3. Cells, cell culture and cell-cycle synchronization

Human cervical carcinoma (HeLa) cells were maintained in Dulbecco's modified Eagle's medium (DMEM) supplemented with 10% fetal bovine serum, penicillin (100 units/ml), and streptomycin (100 μg/ml). These cells were cultured under an atmosphere of 5% CO_2/air at 37 °C. Cell-cycle synchronization was performed by incubating the cells with culture medium containing hydroxyurea (2.5 mM) for 18 h.

2.4. Hela-luciferase stable cell line (HeLa-luc)

HeLa cells were stably transfected with the pGL3 plasmid containing luciferase reporter gene using Lipofectamine PLUS (Invitrogen, Carlsbad, CA, USA). Cells were incubated with lipofectamine PLUS/plasmid for 48 h, and then the medium was replaced by fresh medium containing 800 μg/ml G418 disulfate (Nakalai Tesque Inc., Kyoto, Japan). Antibiotic-resistant colonies were expanded and selected for high luciferase expression after 2 weeks. When HeLa-luc cells were cultured, the cells were maintained in culture medium containing 400 μg/ml G418 disulfate.

2.5. Microinjection

The microinjection study was performed as reported previously [12,14]. Briefly, microinjection was carried out by using a semi-automatic injection system (Eppendorf Transjector 5246) attached to an Eppendorf Micromanipulator 5171 (Eppendorf, Hamburg, Germany) mounted on an inverted microscope (Axiovert 100; Carl Zeiss Co. Ltd., Jena, Germany). Cells were seeded on a glass-base dish (Iwaki, Osaka, Japan) 2 days before microinjection. In the case of cell-cycle synchronization, cells were incubated with hydroxyurea for 18 h before microinjection and all of the subsequent steps were performed in the presence of 2.5 mM hydroxyurea. pDNA was diluted to 3.32 pmol/ml with a 0.5% Rho-dex/H_2O solution as a microinjection marker, and then microinjected into the cytoplasm and nuclei of the cells. Nuclear or cytoplasmic injections were performed under an injection pressure of 50 hPa and a maintenance pressure of 30 hPa, with an injection time of 0.2 s. Just after microinjection, Rho-dex-positive cells were counted using a fluorescence microscope (Axioplan 2; Zeiss). At 24 h post-injection, the number of cells expressing EGFP was counted and the ratio of EGFP-positive cells to Rho-dex-positive cells was calculated.

2.6. Preparation of the MENDs

MENDs were prepared by the lipid hydration method as reported previously [21]. Briefly, pDNA (0.1 mg/ml) was condensed with protamine (0.1 mg/ml) in 10 mM HEPES (pH 7.4), at a nitrogen/phosphate (N/P) ratio of 1.0. A lipid film was prepared in a glass test tube by evaporating a chloroform solution of lipids, containing DOPE, cholesterol, STR-R8, and/or sugar-modified cholesterol (total lipid amount: 82.5 nmol). The prepared lipid film then was hydrated with the condensed DNA solution for 10 min at room temperature; the final lipid concentration was 0.55 mM. After hydration, to complete the lipid coating of the condensed DNA, the tube was sonicated for 1 min in a bath-type sonicator (AU-25C; Aiwa Co., Tokyo, Japan). The diameter and zeta potential of the MEND were determined using an electrophoretic light-scattering spectrophotometer (Zetasizer; Malvern Instruments Ltd., Malvern, WR, UK).

2.7. Transfection and reporter gene assay

Two × 10^4 cells were seeded on a 24-well plate (Corning incorporated, Corning, NY, USA) in 0.5 ml of culture medium 2 days before transfection. A solution of MEND in DMEM solution (0.25 ml, without serum and antibiotics), corresponding to 0.4 μg DNA, was incubated with the cells for 3 h. Then, the medium was replaced with fresh medium containing 10% serum and the cells were incubated for either 3 or 21 h. Cells were washed with 0.25 ml of phosphate-buffered saline (PBS) two times and lysed with 75 μl of reporter lysis buffer (Promega, Madison, WI, USA). In the case of cell-cycle synchronization, the culture medium was changed to fresh medium containing 2.5 mM hydroxyurea, cells were incubated with hydroxyurea for 18 h before transfection, and all of the subsequent steps were performed in the presence of 2.5 mM hydroxyurea. Luciferase activity was initiated by the addition of 50 μl of luciferase assay reagent (Promega) into 20 μl of cell lysate, and was measured by means of a luminometer (Luminescencer-PSN; ATTO, Japan). The amount of protein in the cell lysate was determined using a BCA protein assay kit (PIERCE, Rockford, IL, USA).

2.8. Labeling of the sugar-modified MEND

To examine encapsulation efficiency and intracellular trafficking of sugar-modified MEND, pDNA and the lipid envelope of MEND were labeled. pDNA was labeled with rhodamine by means of Label IT CX-rhodamine reagent (Mirus Corporation, Madison, WI, USA). The lipid envelope was labeled with NBD by using NBD-DOPE (1 mol% of total lipids). Labeled MENDs were prepared as described above.

2.9. Purification of the sugar-modified MEND by sucrose density-gradient centrifugation

To evaluate encapsulation efficiency of sugar-modified MENDs, fluorescence-labeled MENDs were layered on a discontinuous sucrose density gradient (0–60%), and centrifuged at 160,000*g* for 2 h at

20 °C. Aliquots (1 ml) were collected from the top, and the fluorescent intensities of NBD (Excitation: 460 nm, Emission: 534 nm) and CX-rhodamine (Excitation: 576 nm, Emission: 597 nm) in each fraction were measured. To further confirm fluorescence resonance energy transfer (FRET), each fraction was solubilized by 1% sodium dodecyl sulfate (SDS), and the fluorescence intensities were measured. The pDNA-encapsulated fraction was determined by the fraction showed FRET, and the encapsulation efficiency was calculated by the amount of pDNA in the pDNA-encapsulated fractions divided by the total amount of pDNA.

2.10. Visualization of intracellular trafficking of the sugar-modified MEND by confocal microscopy

One $\times 10^5$ cells were seeded on a glass-base dish in 2 ml of culture medium 2 days before transfection. Culture medium was replaced with fresh medium containing 2.5 mM hydroxyurea and the cells were incubated with hydroxyurea for 18 h before transfection. All of the subsequent steps were performed in the presence of 2.5 mM hydroxyurea. A solution of labeled MEND in DMEM solution (2 ml, without serum and antibiotics), corresponding to 2 μg of DNA, was incubated with the cells for 3 h. Then, cell surface MEND-binding was removed by washing three times with 1 ml of PBS containing heparin (20 U/ml). To stain the cell nuclei, the cells were incubated with culture medium containing 5 μg/ml Hoechst 33342 for 10 min at room temperature. After the cells were washed three times with 1 ml of PBS, the culture medium was changed to DMEM/F-12 (Invitrogen, Groningen, Netherlands) and microscopic observation was performed. Confocal images were obtained using a Zeiss LSM 510 META inverted fluorescent microscope equipped with a 63× NA 1.4 Plan-Apochromat objective (Zeiss).

2.11. Quantificative evaluation of intranuclear pDNA by confocal images

Quantification of the confocal images to evaluate the nuclear transfer efficiency was demonstrated using a confocal image-assisted three-dimensionally integrated quantification (CIDIQ) method [31]. 20 *Z*-series images were obtained from top-to-bottom of the cells, and recorded by the Zeiss LSM510 on a PC. Each 8-bit TIFF image was transferred to Image-Pro Plus ver.4.0 (Media Cybernetics Inc., Silver Spring, MD, USA) to quantify the total brightness and pixel area of each r.o.i. For the data analysis, the pixel areas of each cluster in the cytosol: s_i(cyt) and nucleus: s_i(nuc) were separately summed in each X–Y plane, and are denoted as $S'_{Z=j}$(cyt) and $S'_{Z=j}$(nuc), respectively. The values of $S'_{Z=j}$(cyt) and $S'_{Z=j}$(nuc) in each X–Y plane were further summed through all the Z-series of images, and are denoted as S(cyt) and S(nuc), respectively. These values represent the total amount of pDNA in the cytosol and the nucleus in an individual cell. The fractions of pDNA in the nucleus to the totally introduced one F(nuc), were calculated as follows:

$$F(\text{nuc}) = S(\text{nuc})/(S(\text{cyt}) + S(\text{nuc})).$$

2.12. Quantification of intracellular and nuclear-associated pDNA by real-time PCR

One $\times 10^5$ cells were seeded on a 6-well plate (Corning incorporated, Corning, NY, USA) in 2 ml of culture medium 2 days before transfection. Culture medium was replaced with fresh medium containing 2.5 mM hydroxyurea and the cells were incubated with hydroxyurea for 18 h before transfection. All of the subsequent steps were performed in the presence of 2.5 mM hydroxyurea. A solution of MEND in DMEM solution (2 ml, without serum and antibiotics), corresponding to 2 μg of DNA, was incubated with the cells for 3 h. Then, cell surface MEND-binding was removed by washing three times with 1 ml of PBS containing heparin (20 U/ml), the cells were collected by trypsinization (whole cell fraction). To quantify the nuclear pDNA, the fraction was further purified as described previously [32,33]. The collected cells were suspended in 375 μl of CellScrub Buffer (Gene Therapy Systems Inc.), and then 125 μl of cell lysis solution (2% IGEPAL CA630, 40 mM NaCl, 12 mM $MgCl_2$, and 40 mM Tris–HCl, pH 7.4) was added. The suspension was centrifuged at 9200*g* for 2 min at 4 °C, and the supernatant was removed. This operation was repeated three times, and the obtained pellet was used as the nuclear fraction. DNA in the whole cell or nuclear fraction was extracted using a GenElute Mammalian Genomic DNA Miniprep Kit (Sigma-Aldrich, St. Louis, MO, USA) according to the manufacture's protocol, and subjected to real-time PCR with an ABI 7500 real-time system. The reaction mixture consisted of 5 μl of diluted sample DNA solution, 5 pmol of two types of primers (luc(+): GGTCCTATGATTATGTCCGGTTATG and luc(−): ATGTAGCCATCCATCCTTGTCAAT, or Beta-actin-FW694: AGAGGGAAATCGTGCGTGAC and Beta-actin-RV811: CAATAGTGATGACCTGGCCGT) and 12.5 μl of SYBR Green Realtime PCRMaster Mix (TOYOBO Co., Japan). The DNA was denaturized at 95 °C for 15 s, and annealing/extension was performed at 60 °C for 1 min. The denaturation/annealing cycle was repeated 40 times. The amount of pDNA was normalized by the number of nuclei quantified by the copy number of β-actin DNA.

2.13. Inhibition study

To examine the effect of excess free sugars on the transfection activity of sugar-modified MENDs, the transfection experiment was performed in the presence of free sugars: glcNAc, mannose, and galactose. Excess sugars (1, 5, and 20 mM) were added to the MEND solutions during preparation of the transfection samples, and transfection was then performed as described above.

2.14. Statistical analysis

All data are presented as mean ± standard deviation. For comparison of multiple groups, one-way analysis of variance (ANOVA) was performed. When ANOVA was significant, comparisons between the groups were performed using Bonferroni's multiple-comparison *post hoc* test. Differences between groups were considered significant at $P < 0.05$.

3. Results

3.1. Effect of cell-cycle synchronization on transcription and nuclear transfer

To investigate whether nuclear import of pDNA was facilitated via NPC, non-dividing cells were used to evaluate transgene expression. Use of non-dividing cells minimizes NPC-independent nuclear transport that occurs when the nuclear membrane is diminished during mitosis. In the present study, hydroxyurea was used to synchronize the cell cycle at the G_1 phase. Greater than 90% of cells were confirmed by fluorescence-activated cell sorting (FACS) analysis to be synchronized in the G_1 phase [34].

Initially, the effect of cell-cycle synchronization on transcription and nuclear transfer activity was investigated. Luciferase HeLa (HeLa-luc) cells that were stably expressed were synchronized, and luciferase expression at various incubation periods (18, 24, and 42 h) was evaluated first. Compared with non-synchronized HeLa-luc cells, the luciferase expression in synchronized HeLa-luc cells was not affected by the hydroxyurea treatment (Fig. 2A). In addition, the level of luciferase expression in synchronized HeLa-luc cells was exactly same at the different

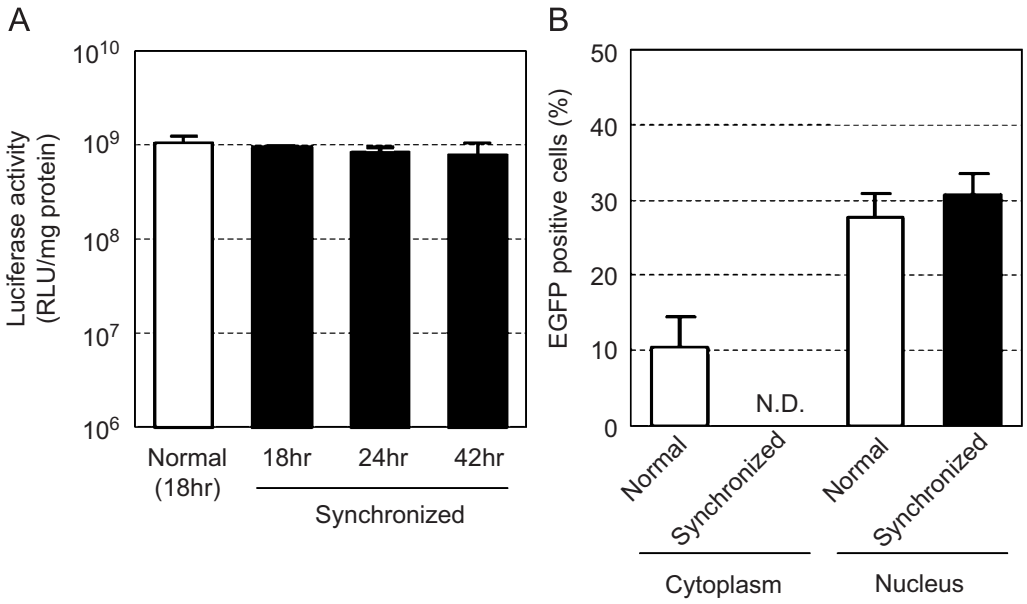

Fig. 2. Effects of cell synchronization on transgene expression. (A) Luciferase stably expressed HeLa cells (HeLa-luc) were incubated with 2.5 mM hydroxyurea for 18, 24, and 42 h, and then luciferase expression was evaluated. (B) Transcription and nuclear transfer efficiencies of exogenous DNA were evaluated by means of microinjection methods. pEGFP-Luc was microinjected into cytoplasm and nuclei of dividing and non-dividing HeLa cells with 0.5% rhodamine-dextran as an injection marker. At 24 h post-microinjection, the ratio of EGFP-expressing to rhodamine-positive cells was determined. Data are presented as mean ± SD of three independent experiments. ND, not detected.

time-points. Then, pDNA encoding EGFP-luciferase fusion protein (EGFP-Luc) was microinjected into the cytoplasm and nuclei of synchronized or non-synchronized HeLa cells and EGFP expression was evaluated (Fig. 2B). Based on the results of intranuclear microinjection, transcription efficiency was not affected by cell-cycle synchronization. Meanwhile, transgene expression after cytoplasmic microinjection was greatly inhibited when mitosis was blocked by hydroxyurea. These results indicated that hydroxyurea treatment specially blocked the nuclear-delivery process without affecting the subsequent transcription processes. Therefore, synchronized cells are useful for the evaluation of NPC-dependent nuclear delivery.

3.2. Physicochemical properties of sugar-modified MENDs

To display and specific sugars (i.e. GlcNAc, mannose, and galactose) on the surface of the lipid envelope, cholesterol derivatives were synthesized as described in Materials and methods (Scheme 1). By the sucrose density gradient centrifugation, it was confirmed that gradient encapsulation efficiencies of sugar-modified MEND and unmodified MEND were approximately 90% regardless of sugar modification or cholesterol content (Table 2). Furthermore, stability of the lipid envelope was controlled by changing the cholesterol content. Physicochemical properties of the different MENDs were compared using dynamic light-scattering. Particle sizes ranged from 180 to 220 nm and the zeta potentials were approximately +40 mV (Table 1). Therefore, it was suggested that neither sugar modification nor cholesterol content affected size or zeta potential of the lipid envelope (Table 2).

3.3. Gene delivery to dividing and non-dividing cells by means of sugar-modified MENDs

First, the effect of sugar modification on transfection activity between dividing and non-dividing cells was compared. Dividing and non-dividing HeLa cells were incubated with MENDs and luciferase activity was measured at 6 h post-transfection (Fig. 3). To control the stability of the lipid envelope, cholesterol content was fixed at 50% of total lipid. In addition, previous reports indicated that the density required for sufficient recognition of certain sugars by lectin is approximately 10% [35–37]. Therefore, for sugar modification, 10% of cholesterol was replaced with sugar-conjugated cholesterol. When the total cholesterol content was 50%, sugar-modified MENDs showed 10- and 20-times higher transfection efficiencies compared with unmodified MEND, in dividing and non-dividing cells, respectively (Fig. 3). However, transgene expression decreased drastically in the absence of STR-R8 (data not shown). Therefore, these results suggest that sugars on the surface of the lipid envelope were involved in nuclear transfer rather than cellular uptake.

Next, the effect of lipid envelope stability on transfection efficiency of sugar-modified MEND was evaluated. Sugar density was fixed at 10% and total cholesterol content was reduced from 50% to 30% and 10%. Transfection efficiency was significantly increased with the lower

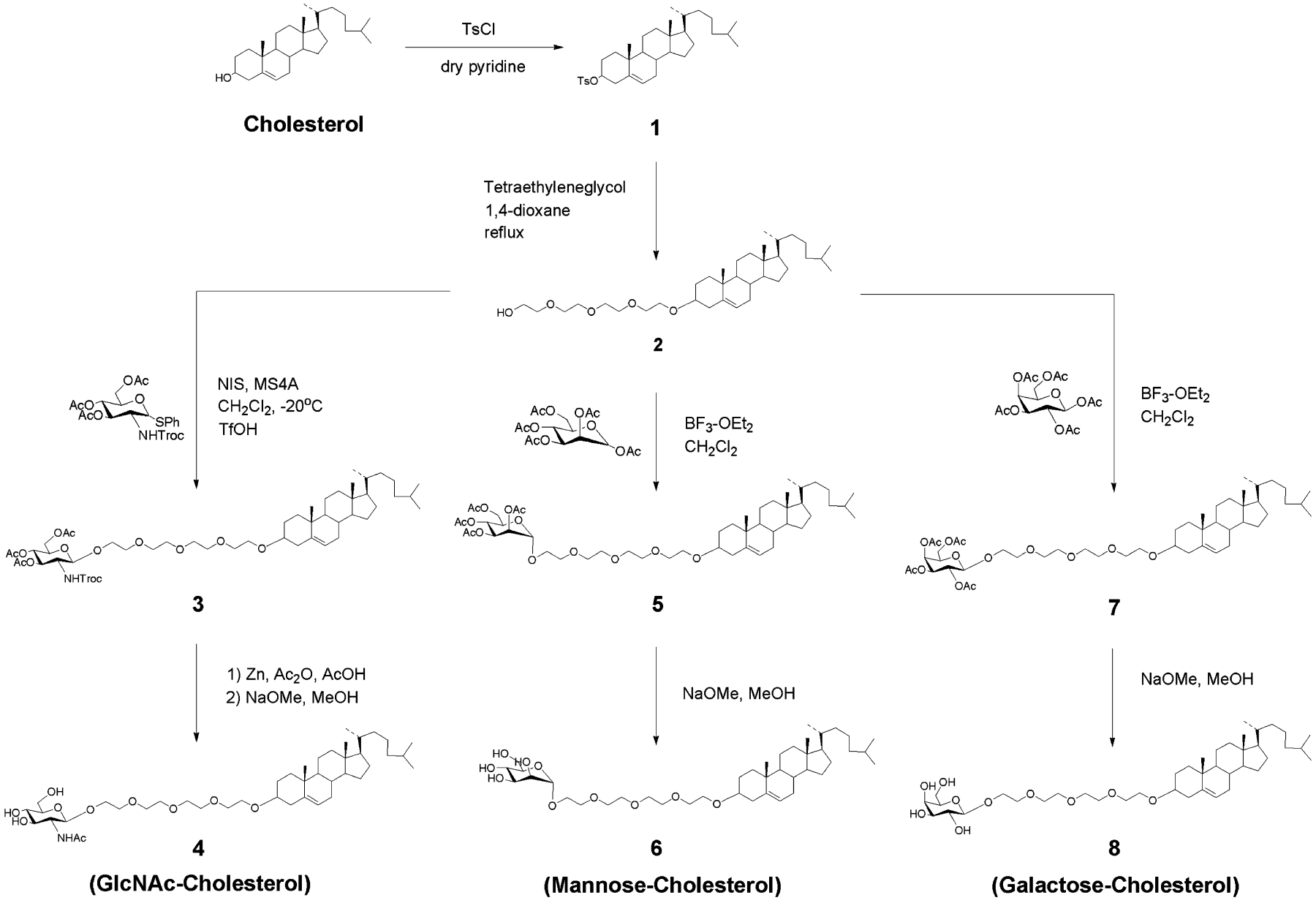

Scheme 1. Synthesis of sugar–cholesterol conjugates.

Table 1
Physicochemical properties of several MENDs used in the present study

Total cholesterol content (%)	Type of cholesterol	Size (nm)	Zeta potential (mV)
50	Cholesterol	213±39	+43.2±2.4
	GlcNAc–cholesterol	213±23	+40.2±0.2
	Mannose–cholesterol	206±24	+43.4±1.8
	Galactose–cholesterol	204±8	+41.4±0.3
30	Cholesterol	183±28	+44.5±4.1
	GlcNAc–cholesterol	180±4	+37.1±1.3
	Mannose–cholesterol	195±9	+38.9±3.6
	Galactose–cholesterol	186±8	+40.2±1.6
10	Cholesterol	194±18	+38.2±3.5
	GlcNAc–cholesterol	180±10	+37.1±1.2
	Mannose–cholesterol	188±13	+35.7±1.5
	Galactose–cholesterol	187±20	+37.2±0.3

Data are the mean±SD of three independent experiments. No significant difference was observed among the four types of MENDs.

Table 2
Encapsulation efficiencies of several MENDs used in the present study

Cholesterol content (%)	Conventional MEND (%)	Sugar-modified MEND (%)
50	85.1	89.4
30	83.7	85.9
10	83.2	81.4

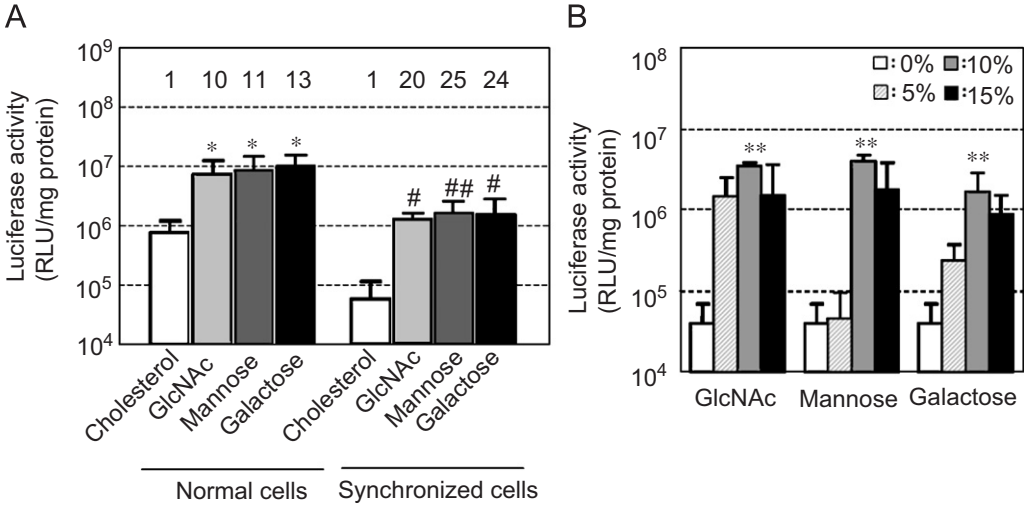

Fig. 3. Transfection activities of sugar-modified MENDs in dividing and non-dividing cells. (A) HeLa cells and synchronized HeLa cells were incubated with sugar-modified MEND (DOPE/cholesterol/sugar–cholesterol/STR-R8 = 50:40:10:5) or unmodified MEND (DOPE/cholesterol/STR-R8 = 50:50:5) for 3 h. After subsequent culture for 3 h in culture medium, luciferase activity was determined. Data are presented as mean±SD of three independent experiments. Numbers on the figure indicate increase in luciferase activity of unmodified MEND (cholesterol). $^{*}P<0.05$ vs control (unmodified MEND) in HeLa cells. $^{\#}P<0.05$, $^{\#\#}P<0.01$ vs control (unmodified MEND) in synchronized HeLa cells. (B) Luciferase activity of sugar-modified MEND in synchronized HeLa cells was determined when sugar density was changed from 0% to 15% (white columns: 0%, striped columns: 5%, grayed bars: 10%, black bars: 15%). The vertical axis shows luciferase activity expressed as relative light units (RLU) per milligram of protein (mg protein). Data are presented as mean±SD of three independent experiments. $^{**}P<0.01$ vs control (unmodified MEND).

cholesterol content. These results suggest that lipid envelope stability is closely related to transfection activity (Fig. 4A and B).

Then, transfection efficiency of sugar-modified MEND at different time-points was evaluated (Fig. 5). Three types of cholesterol content (10%, 30%, and 50%) and three

types of sugar (GlcNAc, mannose, and galactose; cholesterol content was fixed at 10%) were selected. Significant enhancement of transfection efficiency by sugar modification was sustained for a long period (24 h).

3.4. Effects of excess free sugars on transfection efficiency of sugar-modified MENDs

To examine whether sugar modification affected cellular uptake of MEND, transfection efficiencies of sugar-modified MENDs were evaluated in the presence of excess sugar (i.e. GlcNAc, mannose, and galactose) (Fig. 6). Since it is generally accepted that the affinity constant between sugar and lectin ranges from 10^{-4} to 10^{-7} M [38,39], a sugar concentration of 1–20 mM is sufficient to saturate lectin binding. In both dividing and non-dividing cells, for each type of sugar, transfection efficiencies were not inhibited in the presence of excess sugar. This suggests that sugar modification is not involved in cellular uptake. In addition, transfection efficiency of conventional MEND was not affected by excess sugar (Supplementary information S1), and it was suggested that sugars did not affect pDNA transcription efficiency. This finding confirmed that sugar modification affected nuclear transfer, but not cellular uptake.

3.5. Quantitative analysis of cellular uptake and nuclear transfer of sugar-modified MENDs

To quantitatively evaluate cellular uptake and nuclear transfer of sugar-modified MENDs, transfected cells were fractionated and intracellular and nuclear pDNA was quantified by real-time PCR. Cellular pDNA per cell was not affected by sugar modification (Fig. 7A), and nuclear transfer efficiencies of sugar-modified MENDs were significantly enhanced (Fig. 7B). Therefore, sugar modification improved nuclear import of pDNA without affecting cellular uptake.

3.6. Nuclear import of sugar-modified MENDs

To further confirm improved nuclear import of pDNA by sugar modification, fluorescence-labeled MENDs were prepared and intracellular trafficking was visualized by

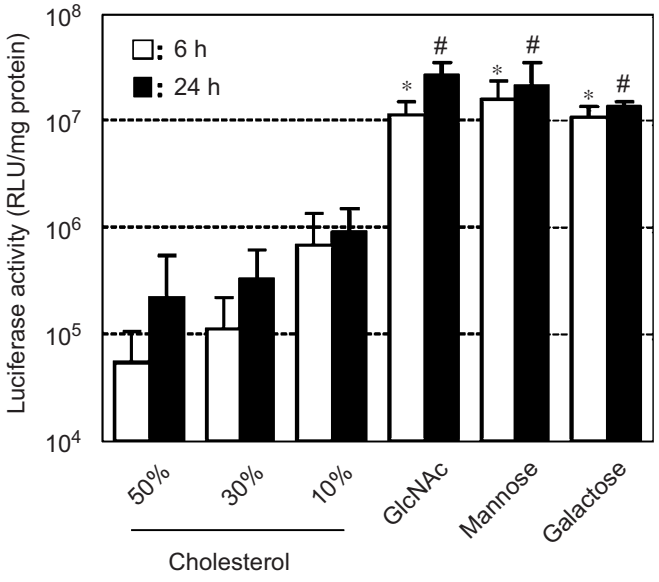

Fig. 5. Comparison of transfection activities of sugar-modified MENDs at various incubation periods. Synchronized HeLa cells were incubated with sugar-modified MEND or unmodified MEND for 3 h. After subsequent culture for 3 or 21 h in culture medium, luciferase activity was determined. The vertical axis shows luciferase activity expressed as relative light units (RLU) per milligram of protein (mg protein). Data are presented as mean ± SD of three independent experiments. $^{*}P<0.05$, $^{\#}P<0.05$ vs total cholesterol: 10% (unmodified MEND) at 6 and 24 h, respectively.

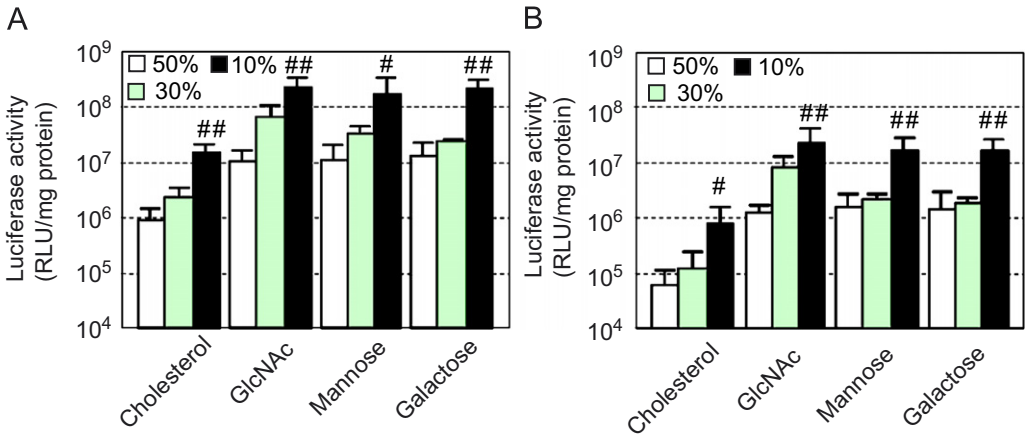

Fig. 4. Effect of cholesterol content of the lipid envelope on transfection activity. HeLa cells (A) and synchronized HeLa cells (B) were incubated with sugar-modified MEND or unmodified MEND for 3 h. After subsequent culture for 3 h in culture medium, luciferase activity was determined. Sugar density was constant (10%), and total cholesterol content was reduced from 50% to 30% and 10%. The vertical axis shows luciferase activity expressed as relative light units (RLU) per milligram of protein (mg protein). Data are presented as mean ± SD of three independent experiments. $^{\#}P<0.05$, $^{\#\#}P<0.01$ vs total cholesterol: 50%.

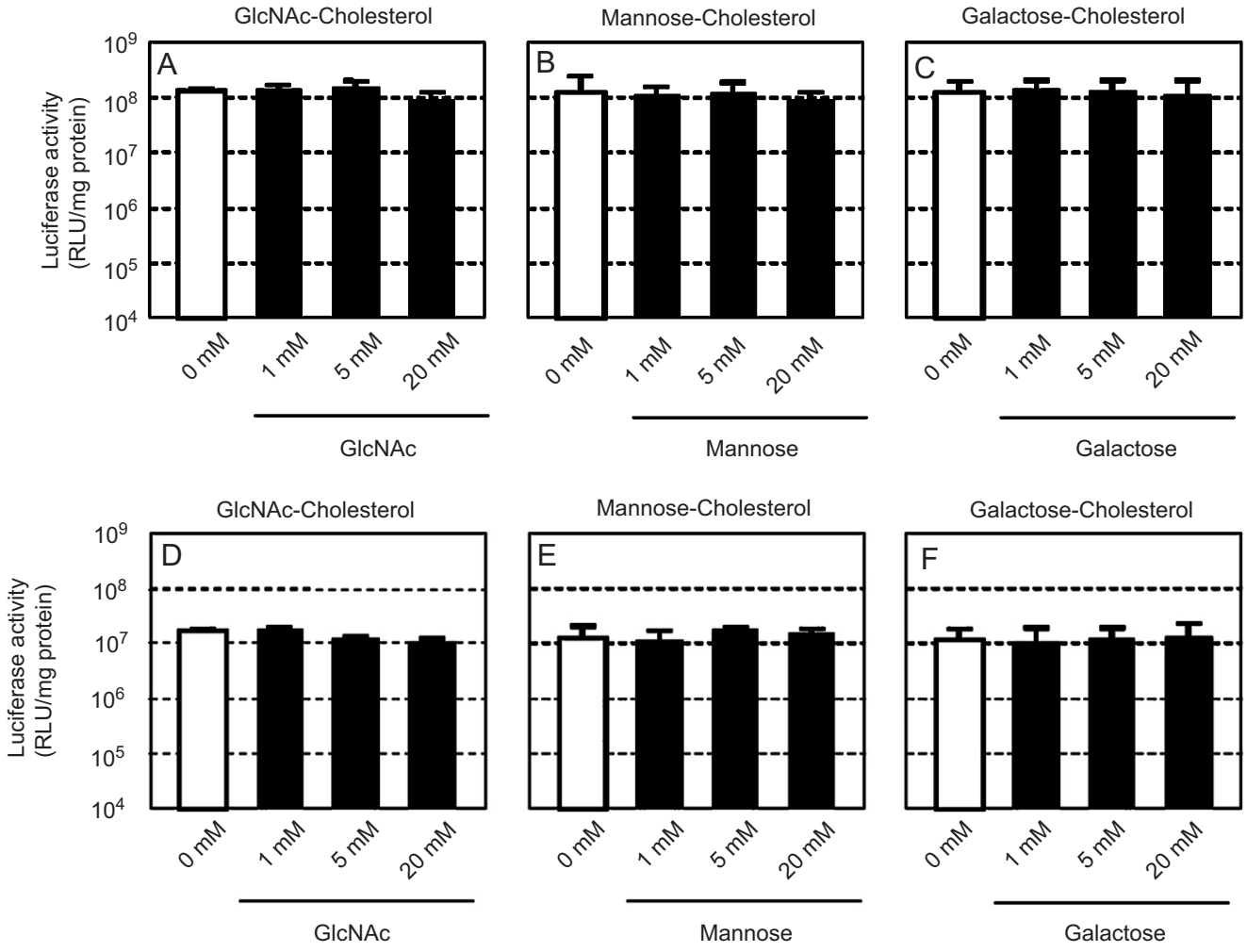

Fig. 6. Effects of excess free sugars on transfection efficiencies of sugar-modified MENDs. HeLa cells (A–C) and synchronized HeLa cells (D–F) were incubated with sugar-modified MEND (DOPE/sugar-cholesterol/STR-R8 = 90:10:5) for 3 h in the presence of excess amount of sugars. After subsequent culture for 3 h in culture medium containing 1–20 mM sugars, luciferase activity was determined. Data are presented as mean ± SD of three independent experiments. No significant difference was observed among the three types of MENDs.

means of confocal laser scanning microscopy. In unmodified MEND, pDNA signals were hardly detected in the nuclei (Fig. 8A). In contrast, pDNA signals detected in the nuclei were drastically increased in all sugar-modified MEND (Fig. 8B–D).

Based on the confocal images, furthermore, these enhanced nuclear pDNA signals were quantified by CIDIQ (Fig. 8E). In unmodified MEND, pDNA signals were not detected in 13 of the analyzed 30 cells. In contrast, nuclear pDNA signals were detected in almost all cells (i.e. 28 or 29 cells to the total cells) in all sugar-modified MEND. In addition, based on the result of quantification, nuclear pDNA signals to the incorporated ones (F(nuc)) in all sugar-modified MENDs were significantly higher than that in unmodified MEND. These results were consistent with the high transfection activity shown in Fig. 4. In summary, enhanced nuclear transfer of pDNA by sugar modification was further demonstrated.

4. Discussion

In the present study, a novel synthetic non-viral vector, which mimics the nuclear gene delivery system of Ad, was developed (Fig. 1B). Ad travels in the cytoplasm in an encapsidated form, and targets the NPC by virtue of the NLS function of capsid proteins [40]. For efficient nuclear targeting, topologic control of NLS is important, as it allows receptor (i.e. importins) recognition. In Ad, NLSs are spontaneously displayed on the Ad particle via a well-ordered assembly of capsid proteins around the DNA core. In the current trials of nuclear delivery via non-viral vectors, NLS was modified using DNA-condensing agents [12,41]. However, when pDNA is condensed with NLS-modified polycations, it is difficult to control the surface display and density of NLS, because cationic amino acids interact with pDNA via strong electrostatic forces. A lipid derivative of a nuclear targeting device was synthesized

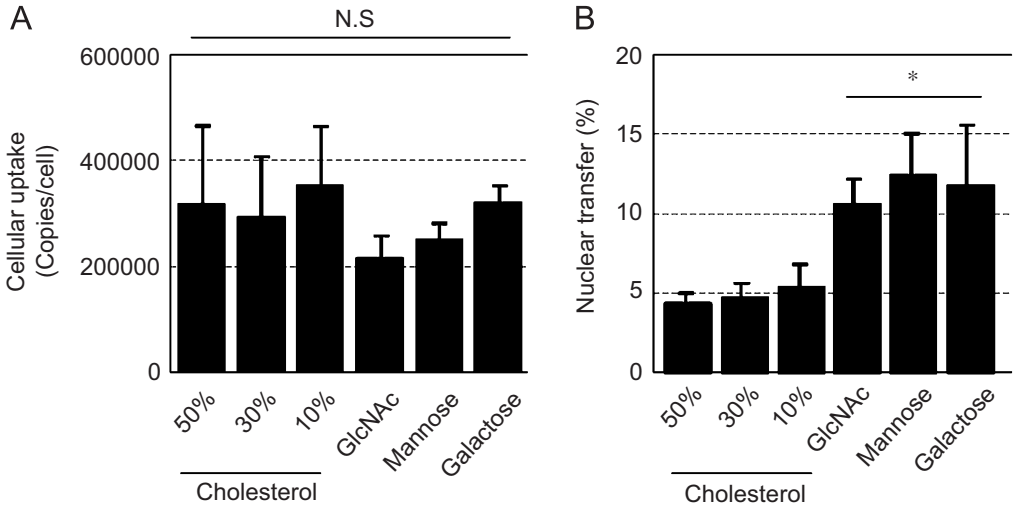

Fig. 7. Quantitative evaluation of cellular uptake and nuclear transfer of sugar-modified MENDs. Synchronized HeLa cells were incubated with sugar-modified MENDs (DOPE/cholesterol or sugar–cholesterol/STR-R8 = 90:10:5) or various cholesterol-containing MENDs (cholesterol content: 10%, 30%, and 50%) for 3 h. After removal of MEND-binding to the cell surface, cell fractionation, and extraction of DNA, luciferase genes in the whole cells and cell nuclei were quantified by real-time PCR. Cellular uptake was calculated as the number of the cellular pDNA normalized by the copy number of β-actin genome (A), and nuclear transfer efficiencies were calculated as the percent of the copy number of nuclear pDNA divided by that of cellular pDNA (B). Data are presented as mean $\pm$ SD of three independent experiments. $^{*}P<0.05$ vs total cholesterol 10% (unmodified MEND). NS, no significant difference.

such that the lipid moiety was incorporated into the envelope structure and the NLS spontaneously oriented outward towards the MEND surface. Moreover, control of NLS density was easily achieved by changing the lipid composition. Sugars were the nuclear targeting device of interest in this study. Nuclear-lectin-mediated gene delivery by means of glycosylated polymers, such as lactosylated polylysine and lactosylated polyethyleneimine recently has been reported [42–48]. In addition, because sugars are neutral and highly soluble in water, it is expected that recognition of surface sugars by lectin is not inhibited by mutual interactions with the lipid envelope.

Generally, in experiments with dividing cells, nuclear delivery of pDNA can be achieved when the nuclear membrane is diminished during mitosis [3,4,6,49,50] Therefore, the contribution of nuclear transport via NPC to total nuclear transport cannot be evaluated. In this study, to exclude the contribution of nuclear transport that occurs as a result of cell division and thereby evaluate nuclear transfer ability of the novel vectors, the cell cycle was synchronized and transgene expression was evaluated within a short time (6 h). For the synchronization, we used hydroxyurea-treated cells in the present study. As shown in Fig. 2A, and in a previous report [31], hydroxyurea had little effect on the expression of GL3 stably expressed HeLa cells under the regulation of a CMV promoter. Therefore, hydroxyurea does not affect the efficiency of the post-nuclear-delivery processes (i.e. transcription and translation). This observation is also supported by Fig. 2B, showing that hydroxyurea treatment did not affect the transgene expression of marker gene (EGFP) after the nuclear microinjection of the EGFP-encoding pDNA). Concerning intracellular trafficking, the effect of the hydroxyurea on the cellular uptake process was investigated previously [31]. When rhodamine-labeled pDNA was transfected to the hydroxyurea-treated or non-treated cells by lipofectaminePLUS, a comparable fluorescence signal was detected in the cell. This suggests that the cellular uptake process is not affected by the hydroxyurea treatment. In contrast, transgene expression efficiency of EGFP after the cytoplasmic microinjection of EGFP-encoding pDNA was drastically decreased by the hydroxyurea treatment. These results collectively indicated that hydroxyurea mainly affects the nuclear-delivery process. In summary, the contribution of non-specific nuclear delivery of DNA during mitosis is negligible in synchronized cells and cell-cycle synchronization is useful for evaluating nuclear transfer via NPC.

Next, the effect of sugar modification on transfection activity was evaluated. In this study, three types of sugars (β-GlcNAc, α-mannose, and β-galactose), were used as nuclear targeting ligands [27,51,52] conjugated with cholesterol. Physicochemical properties of the sugar-modified MENDs did not differ from those of the unmodified MEND (Table 1). In contrast, transfection efficiencies of sugar-modified MENDs were drastically increased compared with unmodified MENDs, in both dividing and non-dividing cells (Fig. 3A). In addition, encapsulation efficiencies of sugar-modified MEND and unmodified MEND were approximately 90% regardless of sugar modification. Therefore, the difference in transfection efficiency was not due to the difference in encapsulation efficiency. These data indicate that sugar modification improved intracellular trafficking of MEND.

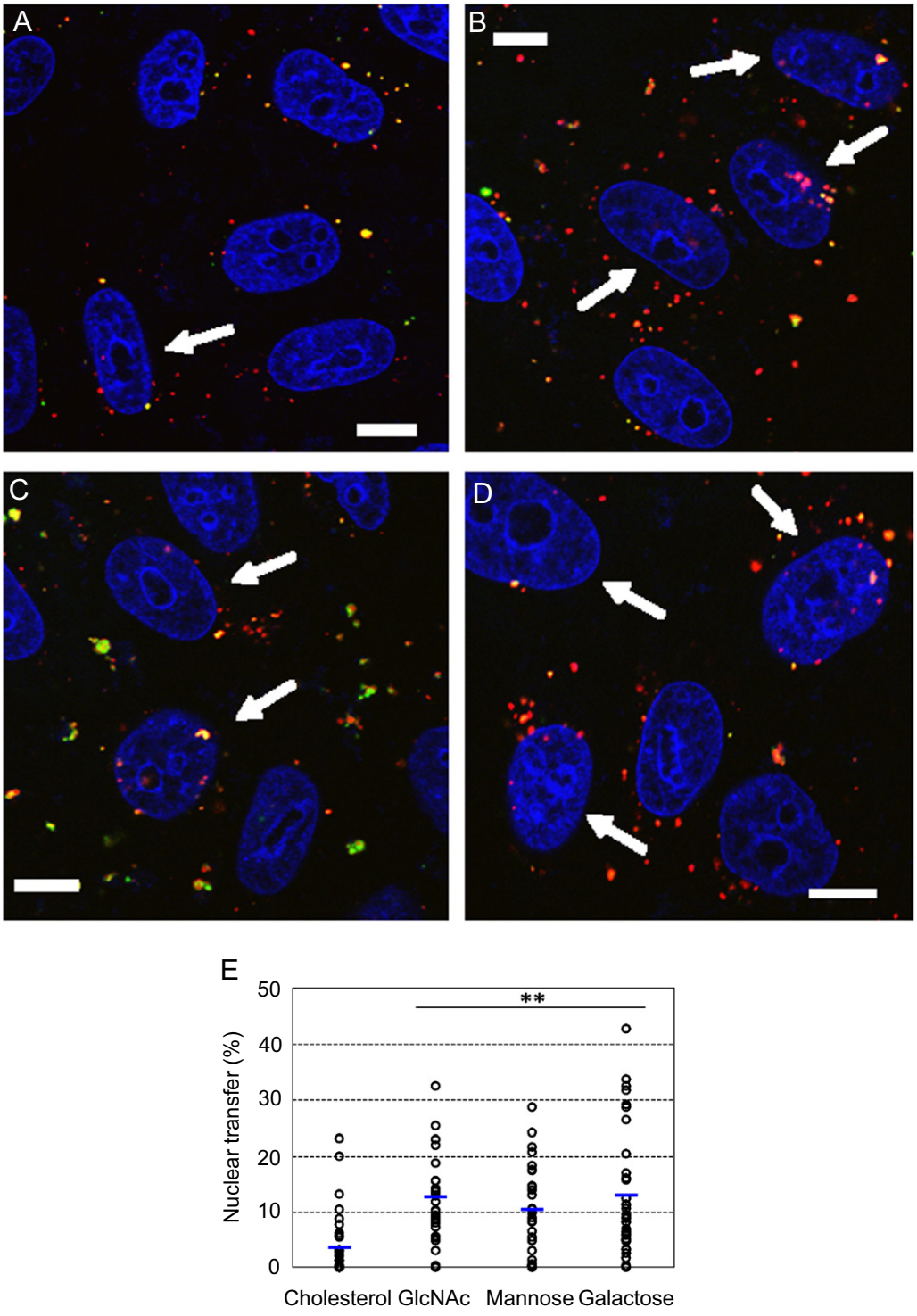

Fig. 8. Confocal microscopy images of intracellular trafficking of sugar-modified MENDs. (A–D) Synchronized HeLa cells were incubated with fluorescence-labeled sugar-modified MEND (DOPE/cholesterol or sugar–cholesterol/STR-R8 = 90:10:5) for 3 h. Intracellular trafficking of sugar-modified MEND (B: GlcNAc, C: Mannose, D: Galactose) was analyzed by means of confocal laser scanning microscopy. As a control, cells were incubated with unmodified MEND (A). Red, green and blue signals indicate pDNA, lipid envelope of the MEND, and nuclei, respectively. Arrows indicate pDNA signals detected in the nuclei. Bars indicate 10 μm. (E) Quantitative evaluation of nuclear transfer of sugar-modified MENDs based on the confocal images. In each group, 30 individual cells were extracted from three independent experiments, and the nuclear fractions of sugar-modified MENDs were quantified by CIDIQ method. $^{**}P<0.01$ vs control (unmodified MEND).

In general, sugars have been used as a tool in gene delivery to enhance the efficiency of cellular uptake. For example, galactose and mannose were specifically recognized by lectins expressed on the cell membrane surface (i.e. asialoglycoprotein receptor and mannose receptor, respectively [53–55]), and their applications for gene delivery have

been reported [42,43,54,56–59]. Transgene expression was considerably diminished in the absence of STR-R8 (data not shown), suggesting that, rather than sugars, R8 is mainly responsible for cellular uptake. This conclusion also was supported by the fact that excess sugar did not inhibit transfection activity (Fig. 6), and that cellular uptake was not enhanced by sugar modification (Fig. 7A).

It is well-accepted that endosomal escape is the second rate-limiting barrier to elevation of transgene expression. Indeed, many reports have demonstrated that transfection activities were enhanced in the presence of chloroquine, which allows gene vectors to escape endosomes and to avoid lysosomal degradation [42–44,57–60]. Direct fusion of the plasma membrane and lipid envelope is one technique for overcoming the endosomal membrane barrier [61]. With direct fusion, transgene expression was improved using an NLS (derived from SV40 large T antigen). However, transgene expression remained to be insufficient, presumably because of poor cellular uptake or cellular toxicity. Therefore, alternative techniques of cytoplasmic delivery are essential. It was previously demonstrated that R8-modified liposome, or MEND, were taken up via macropinocytosis, which is advantageous during gene delivery, as this pathway avoids lysosomal degradation and allows for escape from macropinosomes because of their leaky properties [24,25,62]. Since transfection activity of R8-modified MEND was not changed by chloroquine, endosomal escape was not a rate-limiting barrier in this system (data not shown). In addition, small interfering RNA (siRNA) packaged in R8-MEND showed a high silencing-effect of RNA interference due to the efficient release of siRNA into the cytoplasm [63]. Therefore, it is plausible that improved transgene expression by sugar modification resulting from sugar modification reflected enhanced nuclear transfer efficiency.

In non-dividing cells, transfection activity in sugar-modified MEND was drastically enhanced (14–58-fold) compared with unmodified MEND; enhancement was less prominent in dividing cells (10–25-fold increase), presumably because non-specific nuclear transport during mitosis contributed to overall transfection activity (Figs. 3 and 4). In addition, in sugar-modified MEND, successful nuclear delivery of pDNA was confirmed by confocal laser scanning microscopy (Fig. 7A). Quantitative evaluation of nuclear transfer of pDNA by the CIDIQ method [31] and real-time PCR further supported these results (Figs. 7B and 8). Therefore, sugar modification improved nuclear import of pDNA.

It is very important to address whether the enhancement of the transgene expression was due to the increase of transfixed cells (i.e. cellular uptake) or the increase of the protein production per one cell (i.e. post-cellular uptake processes such as nuclear transfer and intracellular transcription). We previously reported that R8-modified MEND was incorporated in almost all of the cells [33]. In the present study, we also confirmed that cellular uptake of pDNA was observed in all of the analyzed cells regardless of the sugar modification (Fig. 7A). Therefore, it is plausible that enhancement of the transgene expression is due to the increase of the luciferase production per cell. This is supported from the point of view of nuclear delivery (Figs. 7B and 8). To evaluate nuclear transfer efficiency, nuclear pDNA and total cellular pDNA were quantified by real-time PCR, and the nuclear distribution of pDNA was calculated as a nuclear amount of pDNA divided by the total cellular uptake. Furthermore, to investigate the nuclear-delivery efficiency in individual cells, confocal images were further quantified by the CIDIQ method [31]. Nuclear pDNA signals of sugar-modified MENDs were significantly higher than that of unmodified MEND (Fig. 8E). These data collectively indicate that sugar modification increases nuclear delivery of pDNA in individual cells, and results in an increase in luciferase production.

Furthermore, we investigated the sugar-density dependence in the transfection activities (Fig. 3B). Consequently, transfection activity was saturated when sugars were modified at a density of 10% for every sugar in HeLa cells. However, the difference in transfection activity was drastically improved in GlcNAc modification, whereas the transfection activity was only moderately improved in mannose and galactose. These data suggest that sugar density is an important factor for the nuclear delivery, whereas optical density was the same for every sugar (10%), by accident. Based on the results shown in Fig. 3B, it is plausible that sugar density be optimized in each target cell, including non-dividing cells for *in vivo* applications.

In our study, β-galactose-modified MEND showed high transfection activity and nuclear accumulation. This is inconsistent with the previous observations showing that nuclear accumulation of α-galactose-conjugated BSA was not observed [27]. It may be explained by the differences in the anomeric form (i.e. α and β) or by a different density of modification. It is possible that β-conformation of galactose may be favorable as a nuclear targeting signal.

Finally, the effect of lipid envelope stability was evaluated by changing the cholesterol content of the lipid envelope. Transfection activity was drastically enhanced in all of the sugar-modified MENDs depending on reduced cholesterol content (Figs. 4 and 5). It is possible that cholesterol content may affect the structure of MEND or various intracellular trafficking processes (i.e. cellular uptake, nuclear transfer, and intranuclear events). We addressed the stability of MEND in the medium. pDNA and lipid envelope were labeled with CX-rhodamine and NBD, respectively, and the labeled MEND was incubated with the cells. As a result of confocal study, all of the pDNA was co-localized with the lipid envelope at 1 h after the transfection (data not shown), suggesting that MEND was taken up by the cells as intact particles. Then, cellular uptake and nuclear transfer were evaluated by real-time PCR when the cholesterol content was changed. As shown in Fig. 7A, cellular uptake efficiency was not affected by cholesterol content. Meanwhile, nuclear transfer was

apt to increase depending on reduced cholesterol content ($P = 0.059$: 10% vs 50%) (Fig. 7B), suggesting that efficient release of the pDNA/polycation core, in relation to the stability of lipid envelope, is essential for translocation through the NPC and in subsequent transcription processes.

In summary, optimization of the topology of sugars and the stability of the lipid envelope allowed for development of a novel nuclear-delivery system, which mimicked the nuclear-delivery strategy of Ad.

5. Conclusions

In the present study, based on an innovate concept for nuclear gene delivery, we succeeded in developing a novel system for nuclear delivery of pDNA—MEND, in which the vector mimics the viral structure and functions as a nuclear targeting device. In addition, while constructing the MEND, it was determined that several sugars, such as GlcNAc, mannose, and galactose facilitate nuclear transport—but not cellular uptake of pDNA. Furthermore, the results of this study suggest that destabilization of the lipid envelope on the nuclear membrane is closely related to transfection activity and is crucial to enhancing the efficiency of nuclear pDNA delivery. These observations suggest that an optimized, sugar-modified MEND can be a candidate for efficient gene delivery.

Acknowledgments

This work was supported in part by a Grant-in-Aid for Exploratory Research from the Japan Society for the Promotion of Sciences (JSPS) and Grants-in-Aid for Exploratory Research from the Ministry of Education, Culture, Sports, Science and Technology of Japan. The authors would also like to thank Dr. James L. McDonald for his helpful advice in writing the English manuscript.

Appendix A. Supplementary material

The online version of this article contains additional supplementary data. Please visit doi:10.1016/j.biomaterials.2007.09.039.

References

[1] Banks GA, Roselli RJ, Chen R, Giorgio TD. A model for the analysis of nonviral gene therapy. Gene Ther 2003;10:1766–75.
[2] Brunner S, Furtbauer E, Sauer T, Kursa M, Wagner E. Overcoming the nuclear barrier: cell cycle independent nonviral gene transfer with linear polyethylenimine or electroporation. Mol Ther 2002;5:80–6.
[3] Brunner S, Sauer T, Carotta S, Cotten M, Saltik M, Wagner E. Cell cycle dependence of gene transfer by lipoplex, polyplex and recombinant adenovirus. Gene Ther 2000;7:401–7.
[4] Ludtke JJ, Sebestyen MG, Wolff JA. The effect of cell division on the cellular dynamics of microinjected DNA and dextran. Mol Ther 2002;5:579–88.
[5] Seidman MA, Hogan SM, Wendland RL, Worgall S, Crystal RG, Leopold PL. Variation in adenovirus receptor expression and adenovirus vector-mediated transgene expression at defined stages of the cell cycle. Mol Ther 2001;4:13–21.
[6] Tseng WC, Haselton FR, Giorgio TD. Mitosis enhances transgene expression of plasmid delivered by cationic liposomes. Biochim Biophys Acta 1999;1445:53–64.
[7] Ciolina C, Byk G, Blanche F, Thuillier V, Scherman D, Wils P. Coupling of nuclear localization signals to plasmid DNA and specific interaction of the conjugates with importin alpha. Bioconjugate Chem 1999;10:49–55.
[8] Nagasaki T, Myohoji T, Tachibana T, Futaki S, Tamagaki S. Can nuclear localization signals enhance nuclear localization of plasmid DNA? Bioconjugate Chem 2003;14:282–6.
[9] Sebestyen MG, Ludtke JJ, Bassik MC, Zhang G, Budker V, Lukhtanov EA, et al. DNA vector chemistry: the covalent attachment of signal peptides to plasmid DNA. Nat Biotechnol 1998;16:80–5.
[10] Tanimoto M, Kamiya H, Minakawa N, Matsuda A, Harashima H. No enhancement of nuclear entry by direct conjugation of a nuclear localization signal peptide to linearized DNA. Bioconjugate Chem 2003;14:1197–202.
[11] Zanta MA, Belguise-Valladier P, Behr JP. Gene delivery: a single nuclear localization signal peptide is sufficient to carry DNA to the cell nucleus. Proc Natl Acad Sci USA 1999;96:91–6.
[12] Akita H, Tanimoto M, Masuda T, Kogure K, Hama S, Ninomiya K, et al. Evaluation of the nuclear delivery and intra-nuclear transcription of plasmid DNA condensed with micro (mu) and NLS-micro by cytoplasmic and nuclear microinjection: a comparative study with poly-L-lysine. J Gene Med 2006;8:198–206.
[13] Chan CK, Jans DA. Enhancement of polylysine-mediated transferrinfection by nuclear localization sequences: polylysine does not function as a nuclear localization sequence. Hum Gene Ther 1999;10:1695–702.
[14] Masuda T, Akita H, Harashima H. Evaluation of nuclear transfer and transcription of plasmid DNA condensed with protamine by microinjection: the use of a nuclear transfer score. FEBS Lett 2005;579:2143–8.
[15] Ritter W, Plank C, Lausier J, Rudolph C, Zink D, Reinhardt D, et al. A novel transfecting peptide comprising a tetrameric nuclear localization sequence. J Mol Med 2003;81:708–17.
[16] Rudolph C, Plank C, Lausier J, Schillinger U, Muller RH, Rosenecker J. Oligomers of the arginine-rich motif of the HIV-1 TAT protein are capable of transferring plasmid DNA into cells. J Biol Chem 2003;278:11411–8.
[17] Kasamatsu H, Nakanishi A. How do animal DNA viruses get to the nucleus? Annu Rev Microbiol 1998;52:627–86.
[18] Hitt MM, Graham FL. Adenovirus vectors for human gene therapy. Adv Virus Res 2000;55:479–505.
[19] Robbins PD, Ghivizzani SC. Viral vectors for gene therapy. Pharmacol Ther 1998;80:35–47.
[20] Trotman LC, Mosberger N, Fornerod M, Stidwill RP, Greber UF. Import of adenovirus DNA involves the nuclear pore complex receptor CAN/Nup214 and histone H1. Nat Cell Biol 2001;3:1092–100.
[21] Kogure K, Moriguchi R, Sasaki K, Ueno M, Futaki S, Harashima H. Development of a non-viral multifunctional envelope-type nano device by a novel lipid film hydration method. J Control Release 2004;98:317–23.
[22] Hatakeyama H, Akita H, Kogure K, Oishi M, Nagasaki Y, Kihira Y, et al. Development of a novel systemic gene delivery system for cancer therapy with a tumor-specific cleavable PEG-lipid. Gene Ther 2007;14:68–77.
[23] Moriguchi R, Kogure K, Akita H, Futaki S, Miyagishi M, Taira K, et al. A multifunctional envelope-type nano device for novel gene delivery of siRNA plasmids. Int J Pharm 2005;301:277–85.

[24] Khalil IA, Kogure K, Futaki S, Hama S, Akita H, Ueno M, et al. Octaarginine-modified multifunctional envelope-type nanoparticles for gene delivery. Gene Ther 2007;14:682–9.
[25] Khalil IA, Kogure K, Futaki S, Harashima H. High density of octaarginine stimulates macropinocytosis leading to efficient intracellular trafficking for gene expression. J Biol Chem 2006;281:3544–51.
[26] Duverger E, Carpentier V, Roche AC, Monsigny M. Sugar-dependent nuclear import of glycoconjugates from the cytosol. Exp Cell Res 1993;207:197–201.
[27] Duverger E, Pellerin-Mendes C, Mayer R, Roche AC, Monsigny M. Nuclear import of glycoconjugates is distinct from the classical NLS pathway. J Cell Sci 1995;108:1325–32.
[28] Monsigny M, Rondanino C, Duverger E, Fajac I, Roche AC. Glyco-dependent nuclear import of glycoproteins, glycoplexes and glycosylated plasmids. Biochim Biophys Acta 2004;1673:94–103.
[29] Rondanino C, Bousser MT, Monsigny M, Roche AC. Sugar-dependent nuclear import of glycosylated proteins in living cells. Glycobiology 2003;13:509–19.
[30] Futaki S, Ohashi W, Suzuki T, Niwa M, Tanaka S, Ueda K, et al. Stearylated arginine-rich peptides: a new class of transfection systems. Bioconjugate Chem 2001;12:1005–11.
[31] Akita H, Ito R, Khalil IA, Futaki S, Harashima H. Quantitative three-dimensional analysis of the intracellular trafficking of plasmid DNA transfected by a nonviral gene delivery system using confocal laser scanning microscopy. Mol Ther 2004;9:443–51.
[32] Moriguchi R, Kogure K, Iwasa A, Akita H, Harashima H. Non-linear pharmacodynamics in a non-viral gene delivery system: positive non-linear relationship between dose and transfection efficiency. J Control Release 2006;110:605–9.
[33] Iwasa A, Akita H, Khalil IA, Kogure K, Futaki S, Harashima H. Cellular uptake and subsequent intracellular trafficking of R8-liposomes introduced at low temperature. Biochim Biophys Acta 2006;1758:713–20.
[34] Akita H, Ito R, Kamiya H, Kogure K, Harashima H. Cell cycle dependent transcription, a determinant factor of heterogeneity in cationic lipid-mediated transgene expression. J Gene Med 2007;9: 197–207.
[35] Molin K, Fredman P, Svennerholm L. Binding specificities of the lectins PNA, WGA and UEA I to polyvinylchloride-adsorbed glycosphingolipids. FEBS Lett 1986;205:51–5.
[36] Monsigny M, Roche AC, Sene C, Maget-Dana R, Delmotte F. Sugar-lectin interactions: how does wheat-germ agglutinin bind sialoglycoconjugates? Eur J Biochem 1980;104:147–53.
[37] Sato T, Serizawa T, Ohtake F, Nakamura M, Terabayashi T, Kawanishi Y, et al. Quantitative measurements of the interaction between monosialoganglioside monolayers and wheat germ agglutinin (WGA) by a quartz-crystal microbalance. Biochim Biophys Acta 1998;1380:82–92.
[38] Opanasopit P, Shirashi K, Nishikawa M, Yamashita F, Takakura Y, Hashida M. In vivo recognition of mannosylated proteins by hepatic mannose receptors and mannan-binding protein. Am J Physiol 2001;280:G879–89.
[39] De Boeck H, Lis H, van Tilbeurgh H, Sharon N, Loontiens FG. Binding of simple carbohydrates and some of their chromophoric derivatives to soybean agglutinin as followed by titrimetric procedures and stopped flow kinetics. J Biol Chem 1984;259:7067–74.
[40] Meier O, Greber UF. Adenovirus endocytosis. J Gene Med 2003; 5:451–62.
[41] Chan CK, Senden T, Jans DA. Supramolecular structure and nuclear targeting efficiency determine the enhancement of transfection by modified polylysines. Gene Ther 2000;7:1690–7.
[42] Fajac I, Grosse S, Briand P, Monsigny M. Targeting of cell receptors and gene transfer efficiency: a balancing act. Gene Ther 2002;9:740–2.
[43] Fajac I, Thevenot G, Bedouet L, Danel C, Riquet M, Merten M, et al. Uptake of plasmid/glycosylated polymer complexes and gene transfer efficiency in differentiated airway epithelial cells. J Gene Med 2003;5:38–48.
[44] Grosse S, Tremeau-Bravard A, Aron Y, Briand P, Fajac I. Intracellular rate-limiting steps of gene transfer using glycosylated polylysines in cystic fibrosis airway epithelial cells. Gene Ther 2002; 9:1000–7.
[45] Menon RP, Strom M, Hughes RC. Interaction of a novel cysteine and histidine-rich cytoplasmic protein with galectin-3 in a carbohydrate-independent manner. FEBS Lett 2000;470:227–31.
[46] Moutsatsos IK, Wade M, Schindler M, Wang JL. Endogenous lectins from cultured cells: nuclear localization of carbohydrate-binding protein 35 in proliferating 3T3 fibroblasts. Proc Natl Acad Sci USA 1987;84:6452–6.
[47] Rousseau C, Felin M, Doyennette-Moyne MA, Seve AP. CBP70, a glycosylated nuclear lectin. J Cell Biochem 1997;66:370–85.
[48] Guinez C, Morelle W, Michalski JC, Lefebvre T. *O*-GlcNAc glycosylation: a signal for the nuclear transport of cytosolic proteins? Int J Biochem Cell Biol 2005;37:765–74.
[49] Escriou V, Carriere M, Bussone F, Wils P, Scherman D. Critical assessment of the nuclear import of plasmid during cationic lipid-mediated gene transfer. J Gene Med 2001;3:179–87.
[50] Mortimer I, Tam P, MacLachlan I, Graham RW, Saravolac EG, Joshi PB. Cationic lipid-mediated transfection of cells in culture requires mitotic activity. Gene Ther 1999;6:403–11.
[51] Niikura K, Nishio T, Akita H, Matsuo Y, Kamitani R, Kogure K, et al. Accumulation of *O*-GlcNAc-displaying CdTe quantum dots in cells in the presence of ATP. ChemBioChem 2007;8:379–84.
[52] Duverger E, Roche AC, Monsigny M. *N*-acetylglucosamine-dependent nuclear import of neoglycoproteins. Glycobiology 1996;6:381–6.
[53] Bettinger T, Remy JS, Erbacher P. Size reduction of galactosylated PEI/DNA complexes improves lectin-mediated gene transfer into hepatocytes. Bioconjugate Chem 1999;10:558–61.
[54] Diebold SS, Kursa M, Wagner E, Cotten M, Zenke M. Mannose polyethylenimine conjugates for targeted DNA delivery into dendritic cells. J Biol Chem 1999;274:19087–94.
[55] Erbacher P, Bousser MT, Raimond J, Monsigny M, Midoux P, Roche AC. Gene transfer by DNA/glycosylated polylysine complexes into human blood monocyte-derived macrophages. Hum Gene Ther 1996;7:721–9.
[56] Erbacher P, Roche AC, Monsigny M, Midoux P. Glycosylated polylysine/DNA complexes: gene transfer efficiency in relation with the size and the sugar substitution level of glycosylated polylysines and with the plasmid size. Bioconjugate Chem 1995;6:401–10.
[57] Fajac I, Briand P, Monsigny M, Midoux P. Sugar-mediated uptake of glycosylated polylysines and gene transfer into normal and cystic fibrosis airway epithelial cells. Hum Gene Ther 1999; 10:395–406.
[58] Kollen WJ, Midoux P, Erbacher P, Yip A, Roche AC, Monsigny M, et al. Gluconoylated and glycosylated polylysines as vectors for gene transfer into cystic fibrosis airway epithelial cells. Hum Gene Ther 1996;7:1577–86.
[59] Midoux P, Mendes C, Legrand A, Raimond J, Mayer R, Monsigny M, et al. Specific gene transfer mediated by lactosylated poly-L-lysine into hepatoma cells. Nucleic Acids Res 1993; 21:871–8.
[60] Erbacher P, Roche AC, Monsigny M, Midoux P. Putative role of chloroquine in gene transfer into a human hepatoma cell line by DNA/lactosylated polylysine complexes. Exp Cell Res 1996;225: 186–94.
[61] Nakamura T, Moriguchi R, Kogure K, Minoura A, Masuda T, Akita H, et al. Delivery of condensed DNA by liposomal non-viral gene delivery system into nucleus of dendritic cells. Biol Pharm Bull 2006;29:1290–3.
[62] Khalil IA, Kogure K, Akita H, Harashima H. Uptake pathways and subsequent intracellular trafficking in nonviral gene delivery. Pharmacol Rev 2006;58:32–45.
[63] Nakamura Y, Kogure K, Futaki S, Harashima H. Octaarginine-modified multifunctional envelope-type nano device for siRNA. J Control Release 2007;119:360–7.